Journal of Materials Science Research and Reviews

9(3): 1-16, 2022; Article no.JMSRR.86675

Optical Basicity and Electronic Polarisability of Zinc Tellurite Glass System Doped with Sm^{3+} ions

R. A. Tafida [a,b*] , H. I. Midala [a,c], M. Y. Onimisi [b], I. I. Lakin [a,d] and S. B. Adamu [a,e]

[a] Department of Physics, Faculty of Science, Universiti Putra Malaysia, Serdang Selangor, UPM 43400. Malaysia.
[b] Department of Physics, Nigerian Defence Academy, Afaka, PMB 2109, Kaduna, Nigeria.
[c] Department of Science Laboratory Technology, Federal Polytechnic Mubi, Adamawa State, Nigeria.
[d] Physics Department, Kaduna State University, P.M.B 2339, Tafawa Balewa Way Kaduna State, Nigeria.
[e] Department of Physics, Sule Lamido University, Kafin Hausa, Jigawa State, Nigeria.

Authors' contributions

This work was carried out in collaboration among all authors. All authors read and approved the final manuscript.

Article Information

Open Peer Review History:
This journal follows the Advanced Open Peer Review policy. Identity of the Reviewers, Editor(s) and additional Reviewers, peer review comments, different versions of the manuscript, comments of the editors, etc are available here: https://www.sdiarticle5.com/review-history/86675

Original Research Article

Received 10 March 2022
Accepted 12 May 2022
Published 20 May 2022

ABSTRACT

Zinc tellurite glass system doped with samarium oxide were prepared using a melt quenching technique. The analysis of X-ray diffraction (XRD) and Fourier Transform Infrared (FTIR) were employed to obtain the structural properties. The XRD result revealed the amorphous nature of the sample glasses. The density of the glass system increases with increase in dopant. The refractive index was obtained using the proposed relation of Sakka and Dimitrov. The values of theoretical electronic polarisability, polarisability of oxide ion and metallization criterion of the glass system were obtained via the equation of Lorenz-Lorenz. The band gap energy and refractive index based optical basicity were calculated by the Duffy and Ingram relation. The refractive index and energy band gap-based metallization criterion showed an increasing trend with increasing Sm_2O_3 concentration. Urbach energy decreases with an increase in dopant concentration. The decreasing Urbach energy confirmed that the glass samples have a higher tendency to reduce static disorder within its structure. The obtained result showed that the sample glasses have all potentials to be used on optical limiting devices for photonics.

Keywords: Telluride glasses; index of refraction; oxide ion polarisability; optical basicity; electronic polarisability; metallization criterion.

**Corresponding author: Email: tafidajalingo@yahoo.com;*

1. INTRODUCTION

"Tellurium oxide (TeO_2) based glasses are of scientific and technological concern because of their high polarisability and non-linear optical properties" [1]. TeO_2 based glasses have been recommended by many researchers to be used in photonic devices[2]. "Samarium oxide is added as a dopant into the glass network as a result of their lower melting point and good rare-earth ions solubility"[2]. The addition of zinc oxide into the glass composition improves the forming ability of the fabricated samples as well as lower the crystallization rate of tellurite doped glasses [3]. "Zinc tellurite doped glasses are stable and developed a lot of interest from scientist around the world because of their dual important roles as a network modifier and network former respectively"[3]. Recently, Komatsu and Dimitrov (2005) examined the polarisability method of various oxide glasses by taking an estimation on the oxide ion electronic polarisability, optical basicity as well as the metallization criterion based on refractive index and optical energy band gap of the synthesized glass samples. The optical nonlinearity of glass material is the reason behind the electronic polarization of the glass upon exposure to intense light beams and therefore polarisability is the most significant parameter that indicates the non-linearity response of the glass materials and is closely connected to most properties of a materials like conductivity, optical basicity as well as the optical nonlinearity of glass materials [4]. Therefore, "it is strongly suggested to advance the investigation on the optical basicity, metallization criterion and the electronic polarisability of glass materials to estimate the nonlinear optical properties of glass materials"[2]. The main objectives of the study are to identify the effect of samarium oxide concentration on the linear optical properties of the zinc tellurite glass system and also to adopt the proposed polarisability approach of Sakka and Dimitrov by applying the experimental data for band gap as well as refractive index to determine the polarisability, metallization criterion and the optical basicity of the synthesized glass samples using theoretical approach.

2. MATERIALS AND METHODS

2.1 Production of Zinc Tellurite Glasses

Melt quenching technique was employed in the fabrication of samarium oxide doped with zinc tellurite glass system with composition of $[(TeO_2)_{0.7}\ (ZnO)_{\ 0.3}]_{1-x}\ [Sm_2O_3]_{\ x}$, where x = 0.01, 0.02, 0.03, 0.04 and 0.05 molar fraction. To measure the required chemical powders for individual oxide, a digital weighing balance with an accuracy of ± 0.0001g was used. The chemical powders of (Alfa Aesar, 99.99%) tellurium oxide (TeO_2), (Alfa Aesar, 99.99%) zinc oxide (ZnO) and (Alfa Aesar, 99.99%) of samarium (III) oxide (Sm_2O_3) were measured for the glass fabrication process. The weighted chemical powders were mixed thoroughly for about 30 minutes for a homogeneity. The chemical mixture in the alumina crucible was then transferred to the first electric furnace for preheating process at 400^oC for one hour to remove any amount of water vapour or moisture in the chemical mixture. Further, the chemicals were melted for two hours using the second furnace set at 900^o C. The cylindrical steel mould was, then, preheated using the first furnace that was set at 400^o C as the chemicals were melted in the second furnace. After two hours, the molten liquid was poured rapidly into the preheated mould and the melts immediately transferred for annealing process in the first electrical furnace at 400^o C for 1 hour 30 minutes to eliminate air bubbles and thermal strains in the fabricated glasses before the furnace was turned off. The samples were allowed to cool to room temperature before taken out from the furnace and kept in the scintillation vial with silica gel to absorb any vapour. The synthesized glasses were polished with sandpapers of various grades.

2.2 Optical Properties Characterization

For optical properties characterization, the synthesized glasses were cut to a thickness of approximately 2 mm and both the two sides of the glass samples was polished to obtain a flat and smooth surface. The UV-1650PC UV-vis spectrophotometer was used for the characterization of the sample with wavelength ranging from 200 to 2000 nm to get the optical absorption of the glass samples.

2.3 Structural Properties Characterization

For structural properties, the sample was crushed with a plunger before being ground with pestle and mortar to obtain the fine sample powder. The powdered samples were sent for Fourier Transform Infra-Red Spectroscopy (FTIR) and X-ray Diffraction (XRD) for structural investigation of the glass samples respectively.

2.4 Calculation of Glass Sample Density

Density is an important property that is used to explore the structural compactness of tellurite doped glasses [5]. Archimedes principle was used in measuring the density of the present glass samples using electronic densimeter MD-300S (Alfa Mirage). The density measurement for each glass sample was carried out ten (10) times and the average values were taken. The density of the glass sample is obtained using the following relation[6]:

$$\rho_{sample} = \frac{W_{air}}{W_{water}} \times \rho_{water} \quad (1)$$

where *(ρ)* is the density of glass sample in g/cm^3, W represents the weight of sample in air and water in g and cm^3 respectively.

2.5 Analysis of X-ray Diffraction (XRD)

X-ray diffraction (XRD) analysis is a technique mainly used for phase identification of amorphous and crystalline materials. The powdered portion of the glass samples was used to carry out the XRD analysis in the range $20 < 2\theta < 80$ as presented in Fig. 2. The coefficient of optical absorption $\alpha(\omega)$ for the present glass system is realized using the absorbance values obtained from UV-Vis spectroscopy using the following equation:

$$\alpha(\omega) = 2.303\left(\frac{A}{d}\right) \quad (2)$$

The symbol *d* represents the sample thickness in cm, *A* is the absorbance obtained from UV- Vis result. Mott and Davis proposed affiliation among the absorption coefficient and photon energy to obtain the calculation for a direct and indirect transition that exists in the band gap. The relationship as recommended by Mott and Davis is presented in the following equation [15].

$$\alpha(\omega) = \frac{B\left(\hbar\omega - E_{opt}\right)^n}{(\hbar\omega)} \quad (3)$$

The symbol *B* represents the band trailing parameter, the samples photon energy is denoted by *ħω*, *n* is the determining factor for the type of optical transition that exist in the materials and is constant with values of 1/2 and 2 for both indirect and direct forbidden transitions respectively [16].Urbach energy *(ΔE)* of glass materials indicates the amount of disorder of the material and can be obtained using the following relation:

$$\alpha(\omega) = \beta exp\left(\frac{\hbar\omega}{\Delta E}\right) \quad (4)$$

where *ħ* is the reduced plank constant, *β* is constant, *ω* represents photon frequency and *ΔE* is the Urbach energy of the synthesized glass system [18]. The refractive index of the glass samples is calculated using the optical energy band gap values and the proposed equation of Dimitrov and Sakka [21].

$$\frac{n^2-1}{n^2+2} = 1 - \sqrt{\frac{E_{opt}}{20}} \quad (5)$$

where *n* is the index of refraction of the glass system, Eopt represents the indirect energy band gap of the synthesized glasses. Electronic polarisability of tellurite glasses describes the extent of the electron responding to the electric field and it can be obtained using the following equation:

$$\alpha_e = \frac{3(n^2 - 1)}{4\pi N_A(n^2 + 2)} \quad (6)$$

where α_e represents the electronic polarisability, *n* is the index of refraction of the fabricated glasses and N_A is Avogadro's number of the glass system. Oxide ion electronic polarisability *(* α_{o2-}*)* can be calculated based on two independent initial values that are, the energy band gap, E_g and the linear index of refraction, *n* of a glass material as shown in equation 7 and 8.

$$\alpha_{O2} - (n) = \left[\left(\frac{R_m}{2.52}\right) - \sum \alpha_i\right](No_{2^-})^{-1} \quad (7)$$

$$\alpha_{O2} - (E_{opt}) = \left[\left(\frac{V_m}{2.52}\right)\left(1 - \sqrt{\frac{E_{opt}}{20}}\right) - \sum \alpha_i\right](No_{2^-})^{-1} \quad (8)$$

where $\alpha_{o2-}(n)$ is the oxide ion electronic polarisability based on refractive index, $\alpha_{o2-}(Eg)$ is the band gap energy-based oxide ion electronic polarisability, $\sum \alpha i$ stands for molar cation electronic polarisability and the number of oxide ions in the glass system based on the chemical formula of the glass is denoted by No_{2^-}. Theoretically, the optical basicity of the multi-component glass system can be

determined using the equation proposed by Ingram and Duffy (1992).

$$\Lambda_{th} = X_1\Lambda_1 + X_2\Lambda_2 + X_3\Lambda_3 + \cdots + X_n\Lambda_n \quad (9)$$

where $X_1, X_2, X_3, \ldots, X_n$ represent the equivalent segments based on the amount of oxygen of each oxide contributes to the glass network and $\Lambda_1, \Lambda_2 \ldots \Lambda_n$ is the representation of optical basicity assigned to each oxide in the glass network [27]

The optical basicity alternative approach has been established by Duffy (1992) whereby it can be determined using oxide ion polarisability values based on an index of refraction, *n* and band gap energy, E_{opt} [28].

$$\Lambda = 1.67\left(1 - \left(\frac{1}{\alpha_{O^{2-}}}\right)\right) \quad (10)$$

The relation for the metallization criterion of the glass system is determined by subtracting the prediction of $R_m/V_m = 1$.

$$M = 1 - \left(\frac{R_m}{V_m}\right) \quad (11)$$

The metallization criterion based on refractive index, $M(n_o)$ and optical energy gap, $M(E_g)$ of the glass system is obtained as proposed by Sakka and Dimitrov [21].

$$M(n_o) = 1 - \left[\frac{(n_o^2 - 1)}{(n_o^2 + 2)}\right] \quad (12)$$

$$M(E_g) = \sqrt{\frac{E_g}{20}} \quad (13)$$

3. RESULTS AND DISCUSSION

3.1 Density Measurement

Table 1 listed the density values of the glass system while Fig. 2 has depicted the graph of density with various concentration of samarium oxide. The density values increase from 5.041 to 5.300 g/cm^3 as the concentration of Sm_2O_3 increases. The increasing density values can be attributed to the replacement of glass former tellurium oxide with smaller atomic mass (Z_{Te} =127.6 gmol^{-1}) by the dopant samarium, with a larger atomic mass (Z_{Sm} = 150.36 gmol^{-1}) in the glass system [7].

Table 1. Density for $[(TeO_2)_{0.7}\ (ZnO)_{0.3}]_{1-x}\ [Sm_2O_3]_x$ glasses

Molar fraction (Sm_2O_3)	Density (g/cm^3) [±0.045]
0.01	5.041
0.02	5.093
0.03	5.124
0.04	5.214
0.05	5.300

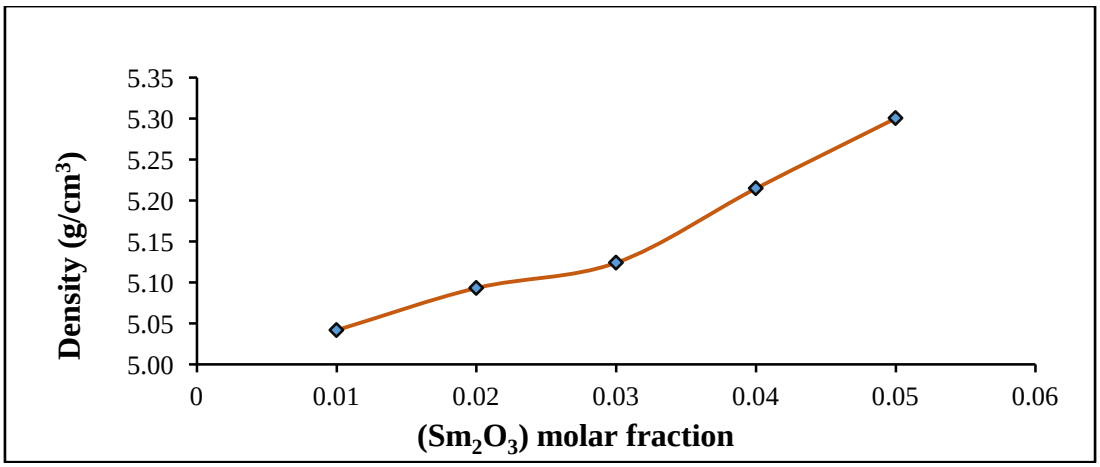

Fig. 1. Plot of density for $[(TeO_2)_{0.7}\ (ZnO)_{0.3}]_{1-x}\ [Sm_2O_3]_x$ glasses

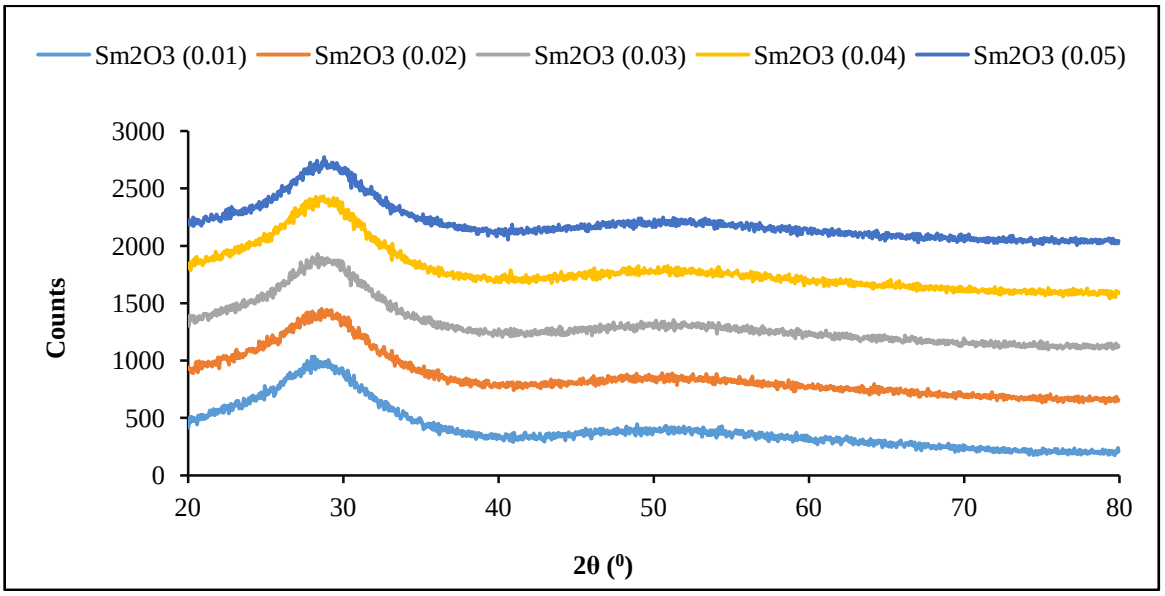

Fig. 2. Plot of X-ray diffraction pattern for $[(TeO_2)_{0.7}\ (ZnO)_{\ 0.3}]_{1-x}\ [Sm_2O_3]_{\ x}$ glasses

"The XRD results show non-appearance of sharp absorption peaks in the spectra but a broad hump which confirms the non-crystalline nature of the glass samples" [2].

3.2 Fourier Transform Infrared Spectroscopy (FTIR)

"Technique of Fourier transform infrared (FTIR) provide details information about the local arrangement, structure as well as functional groups in non-crystalline and crystalline materials" [8]. "The FTIR spectra were recorded in the range 280-4000 cm^{-1}. The absorption band as recorded for FTIR at 600-650 cm^{-1} is assigned to the functional vibration of trigonal bipyramid, TeO_4 in the glass system" [9]. Therefore, the formation of TeO_4 in the present glasses leads to more tightening of the glass structure due to the formation of bridging oxygen [10]. The TeO_4 formation at the expense of TeO_3 indicates the possible presence of Te-O-Zn bonds in the fabricated glasses. The creation of Te-O-Zn might be caused by ZnO which goes into the glass network as a modifier and breaks up of Te-O-Te bonds in the glass system [5]. The disappearance of the bands at wavenumber ranging from 400 to 550 cm^{-1} for ZnO in the fabricated samples is an indication that zinc lattice has been broken down [3]. "The absorption spectra were further deconvoluted to obtain additional information regarding the decrement and increment for every structural unit using Origin 6.0 software. The deconvolution result presented four different absorption bands that can be assigned to tellurite, zinc oxide and Sm_2O_3 structural units in that order. In general, the areas for TeO_4 and TeO_3 structural units increases after the progression. This can be related to the structural redisposition process and breaking of bonds that occur in the glass network" [11] as well as the process of ionization and atomic displacement that happen in the glass matrix. Tables 2 and 3 present the assignment and the deconvolution band centre and band area at different concentration of dopants as depicted in Figs. 3 and 4 respectively.

Table 2. Infrared transmission bands assignment for $[(TeO_2)_{0.7}\ (ZnO)_{\ 0.3}]_{1-x}\ [Sm_2O_3]_{\ x}$ glasses

SM Molar Fraction	Measurement (Infrared transmission band assignment) Stretching Vibrations of Te-O bonds in TeO_4 units [5].
0.01	600cm^{-1}
0.02	603 cm^{-1}
0.03	606 cm^{-1}
0.04	608 cm^{-1}
0.05	650 cm^{-1}

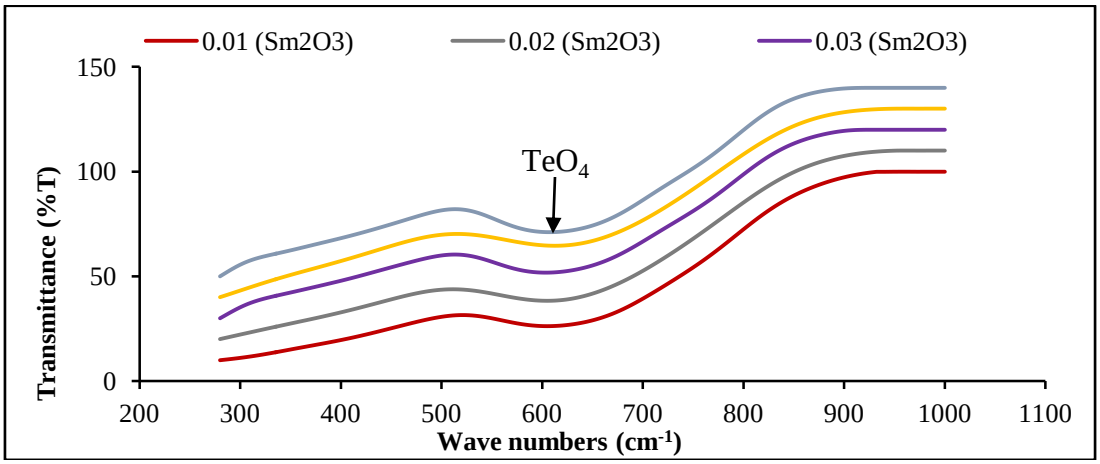

Fig. 3. Plot of FTIR spectra for $[(TeO_2)_{0.7}\ (ZnO)_{\ 0.3}]_{1-x}\ [Sm_2O_3]_{\ x}$ glasses

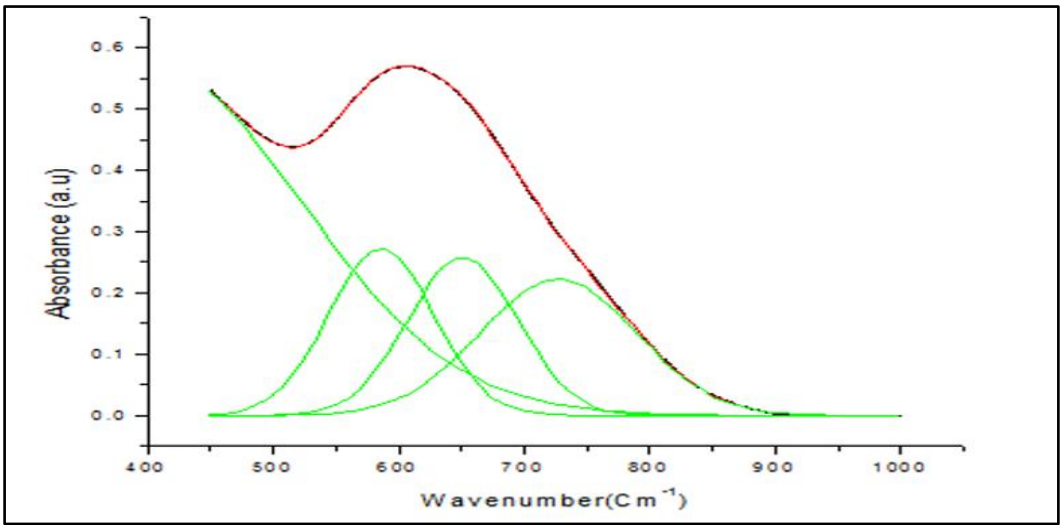

Fig. 4. Spectra deconvolution for $[(TeO_2)_{0.7}\ (ZnO)_{\ 0.3}]_{1-x}\ [Sm_2O_3]_{\ x}$ glasses (0.02)

Table 3. Band area (A), Band Centre (B) and assignments of $[(TeO_2)_{0.7}\ (ZnO)_{\ 0.3}]_{1-x}\ [Sm_2O_3]_{\ x}$ glasses

Molar fraction (Sm_2O_3)	Band Centre, B (cm^{-1}) and band area, A (%)				
0.01	B	417.7	580.3	621.7	746.7
	A	73.9	56.3	49.9	20.3
0.02	B	419.6	562.3	625.8	743.1
	A	57.8	46.6	47.8	18.9
0.03	B	397.2	586.2	681.2	727.2
	A	180.7	28.7	28.2	34.7
0.04	B	282.1	499.7	620.1	728.4
	A	191.7	50.1	46.8	25.0
0.05	B	411.5	586.1	650.4	759.8
	A	73.7	48.5	43.7	9.6
Assignment	Stretching mode of (Sm_2O_3)[8]		Stretching mode of ZnO[7]	Starching mode of TeO_3[13]	TeO_4 trigonal bipyramid[5]

4. OPTICAL ABSORPTION, BAND GAP ENERGY AND URBACH ENERGY

"The optical absorption of glass materials and the absorption edge are of significant importance mainly for the investigation of the transitions that are induced in the glass materials and also to obtain information regarding the band structure and the optical energy gap of non-crystalline" [14]. "The decrement of the absorption coefficient with increasing wavelength is observed. The existence of a non-sharply defined fundamental absorption edge is because of the amorphous nature of the glass samples. As the amount of samarium oxide increases in the glass network, the fundamental absorption edge appears to shift to a longer wavelength as more dopants are added. The shifting of the absorption edge can be ascribed by the increase in the rigidity of the glass samples as the concentration of dopant increases" [3]. There exist seven absorption bands in the spectra located at 405, 482, 960, 1091, 1236, 1389 and 1495 nm. These absorption bands are assigned to the ground state $^6H_{5/2}$ to excited states $^4F_{7/2,}$ $^4I_{9/2}$, $^6F_{11/2}$, $^6F_{9/2}$, $^6F_{7/2}$, $^6F_{5/2}$, and $^6F_{3/2}$ transitions respectively. The absorption spectra for the present glasses is depicted in Fig. 5.

"Both direct and indirect optical band gaps exhibit an increasing trend from 3.409 to 3.702 eV and 2.785 to 2.986 eV with an increase in dopants content. Generally from the literature, the band gap energy of glass materials for direct and indirect transition is determined by the changes in the structure of the samples when a modifier oxide is added to the glass matrix" [2]. "The increasing trend as observed for band gap energy can be because of the decrease in the amount of non-bridging oxygen (NBOs) in the glass system". [17]. "The amount of NBOs reduces due to the increasing number of oxygen anions in the glass system"[2]. The plot of $(\alpha\hbar\omega)^{½}$ for indirect band gap, $(\alpha\hbar\omega)^{2}$ for direct band gap, direct and indirect band gap and Tauc's plot indirect band gap are presented in Figs. 6, 7, 8 and 9 listed in Table 4.

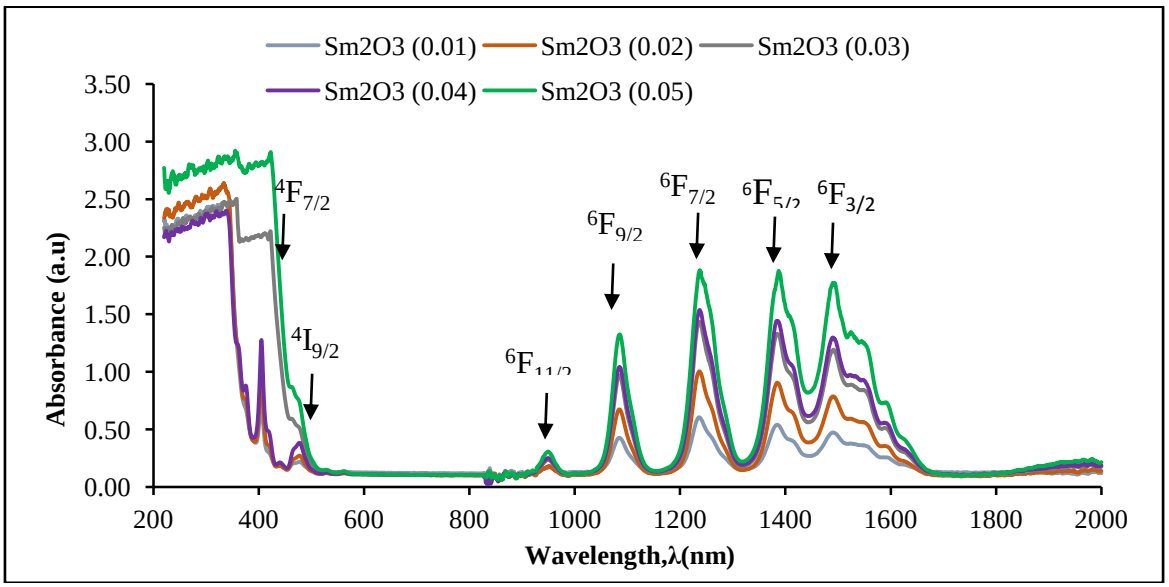

Fig. 5. Plot of optical absorption spectra for $[(TeO_2)_{0.7}$ $(ZnO)_{0.3}]_{1-x}$ $[Sm_2O_3]_x$ glasses

Table 4. Indirect band gap (E^1_{opt}), Direct band gap (E^2_{opt}) and Urbach energy (ΔE) for $[(TeO_2)_{0.7}$ $(ZnO)_{0.3}]_{1-x}$ $[Sm_2O_3]_x$ glasses

Molar fraction (Sm_2O_3)	Indirect band gap E^1_{opt}(eV) [±0.037]	Direct band gap, E^2_{opt} (eV) [±0.056]	Urbach energy ΔE (eV)
0.01	2.785	3.409	0.248
0.02	2.846	3.463	0.231
0.03	2.927	3.507	0.221
0.04	2.957	3.654	0.218
0.05	2.986	3.702	0.207

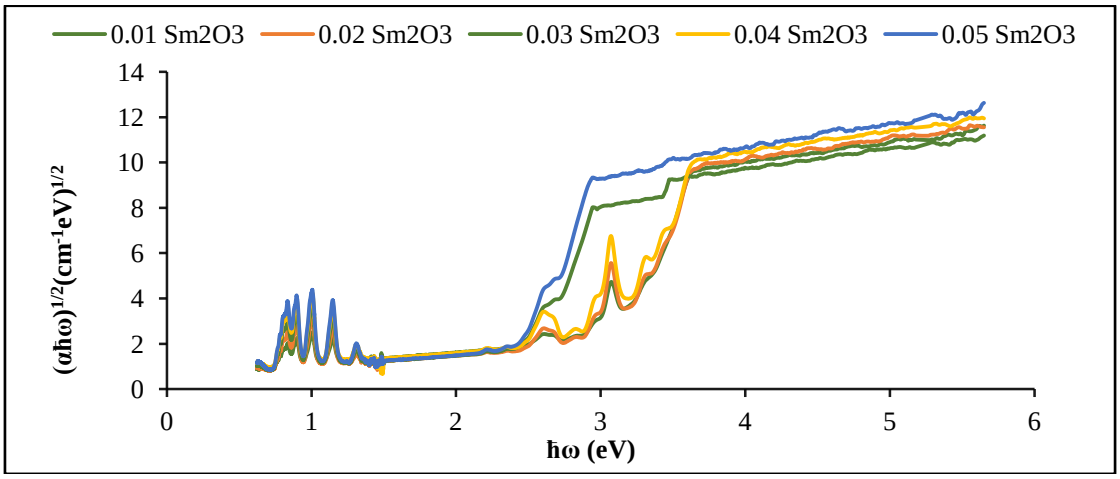

Fig. 6. Plot of $(\alpha\hbar\omega)^{1/2}$ against $\hbar\omega$ for $[(TeO_2)_{0.7}(ZnO)_{0.3}]_{1-x}[Sm_2O_3]_x$ glasses

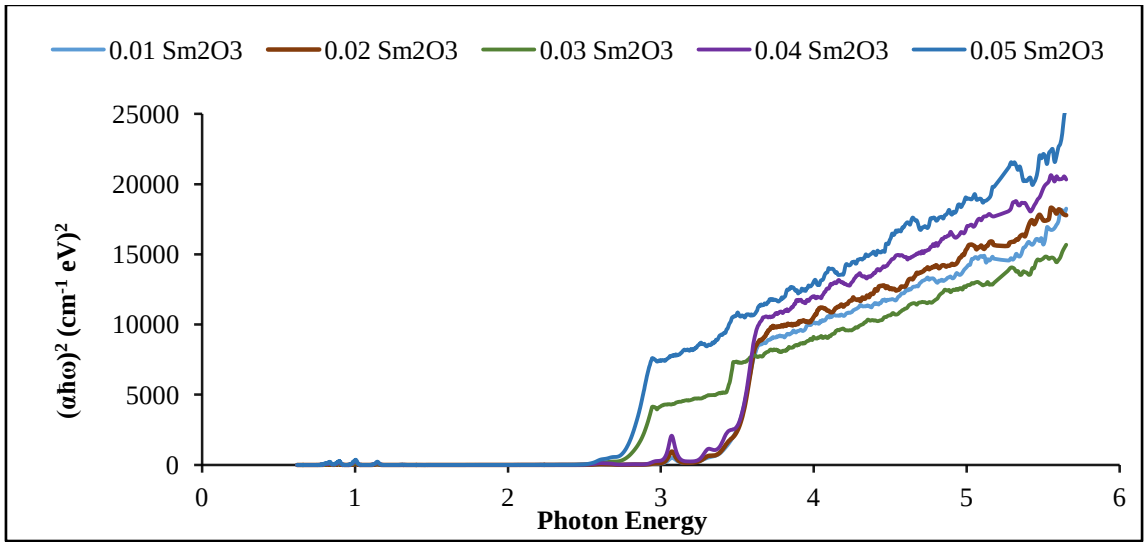

Fig. 7. Plot of $(\alpha\hbar\omega)^2$ against $\hbar\omega$ for $[(TeO_2)_{0.7}(ZnO)_{0.3}]_{1-x}[Sm_2O_3]_x$ glasses

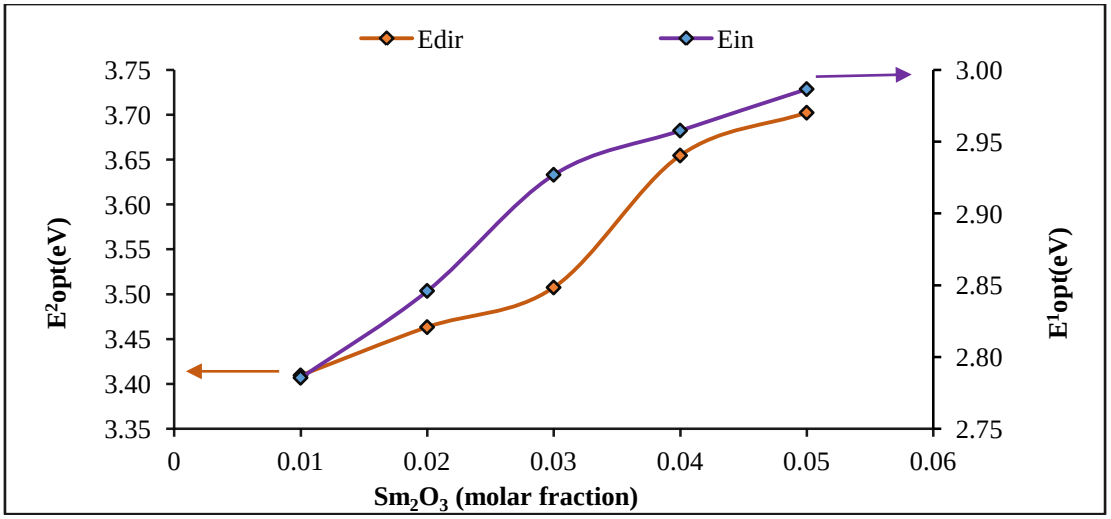

Fig. 8. Direct and indirect band gap for $[(TeO_2)_{0.7}(ZnO)_{0.3}]_{1-x}[Sm_2O_3]_x$ glasses

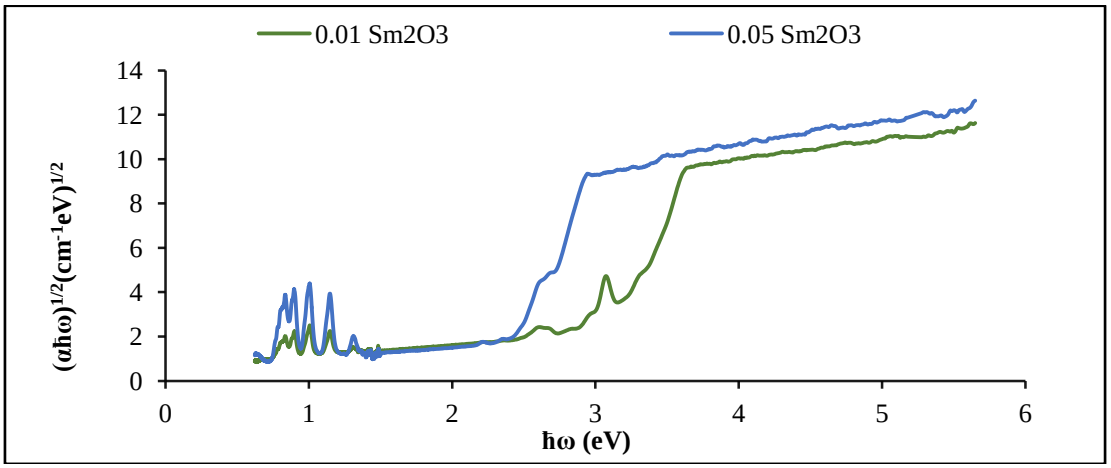

Fig. 9. Tauc's plot indirect band gap for $[(TeO_2)_{0.7}\ (ZnO)_{\ 0.3}]_{1-x}\ [Sm_2O_3]_{\ x}$ glasses

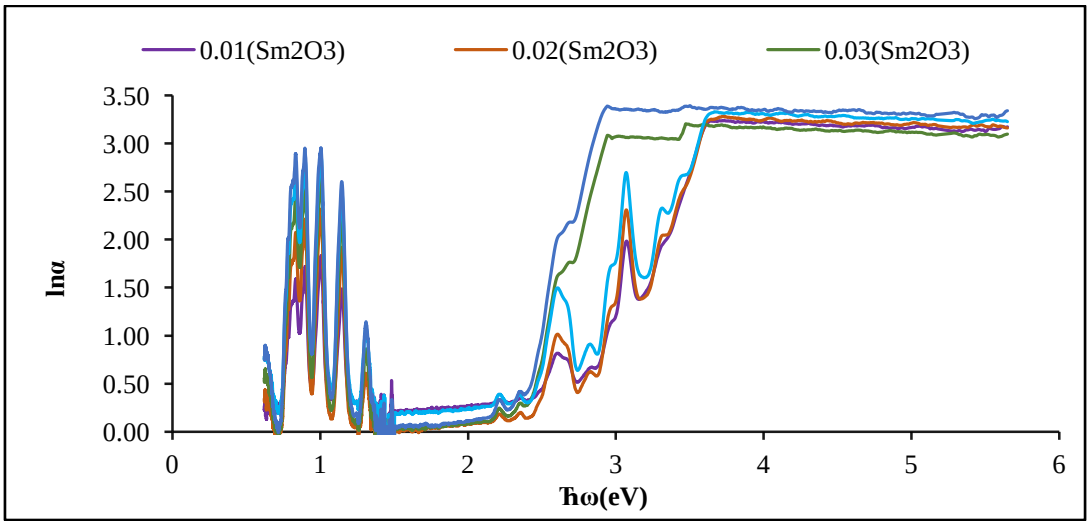

Fig. 10. Plot of (lnα) against (ħω) for $[(TeO_2)_{0.7}\ (ZnO)_{\ 0.3}]_{1-x}\ [Sm_2O_3]_{\ x}$ glasses

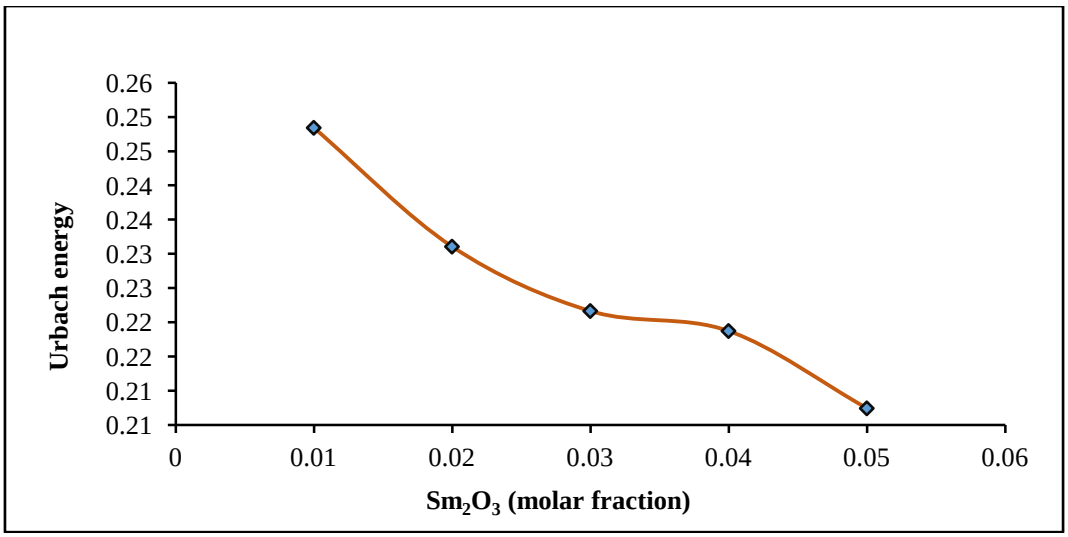

Fig. 11. Plot of Urbach energy for $[(TeO_2)_{0.7}\ (ZnO)_{\ 0.3}]_{1-x}\ [Sm_2O_3]_{\ x}$ glasses

In this work, "Urbach energy is obtained using the reciprocal of the slope of the *ln* (*α)* against (*ħω)* plot. The Urbach energy values show a decreasing trend with an increase in dopant concentration". [12]. "The reduction in Urbach energy with increasing Sm_2O_3 content is attributed to the decrease in the degree of disorderliness in the glass network structure"[19]. The data of Urbach energy are listed in Table 4 and presented in Figs. 10 and 11 respectively.

5. REFRACTIVE INDEX AND ELECTRONIC POLARISABILITY

"The index of refraction of a glass material is one of the most important optical features" [4]. The index of refraction values of glass materials can be used to decide how suitable the glass material is to be applied in optical devices [20]. A lot of researchers examined how the index of refraction can be related to the composition of a glass material [8]. The index of refraction of a glass material is closely associated with the polarisability and the density of the component ions [22]. The refractive index and electronic polarisability exhibit a generally decreasing trend as listed in Table 5 presented in Figures 12 and 13. This can be as a result of the decrease in the amount of NBOs in the glass matrix [5] [23]. This can also be related to the decreasing amount of high polarisability NBOs in the sample glasses.

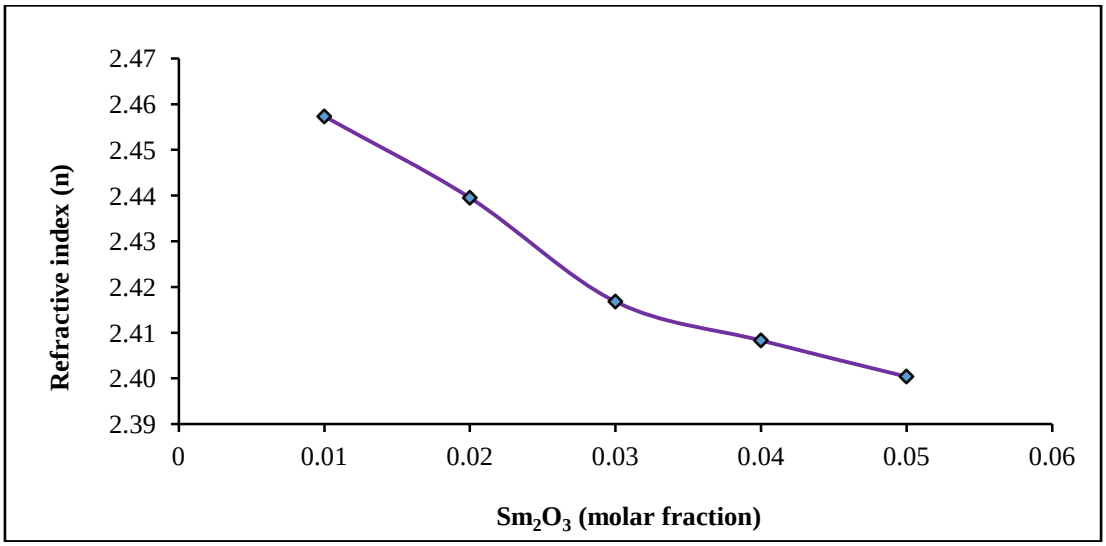

Fig. 12. Plot of refractive index for $[(TeO_2)_{0.7}\ (ZnO)_{0.3}]_{1-x}\ [Sm_2O_3]_x$ glasses

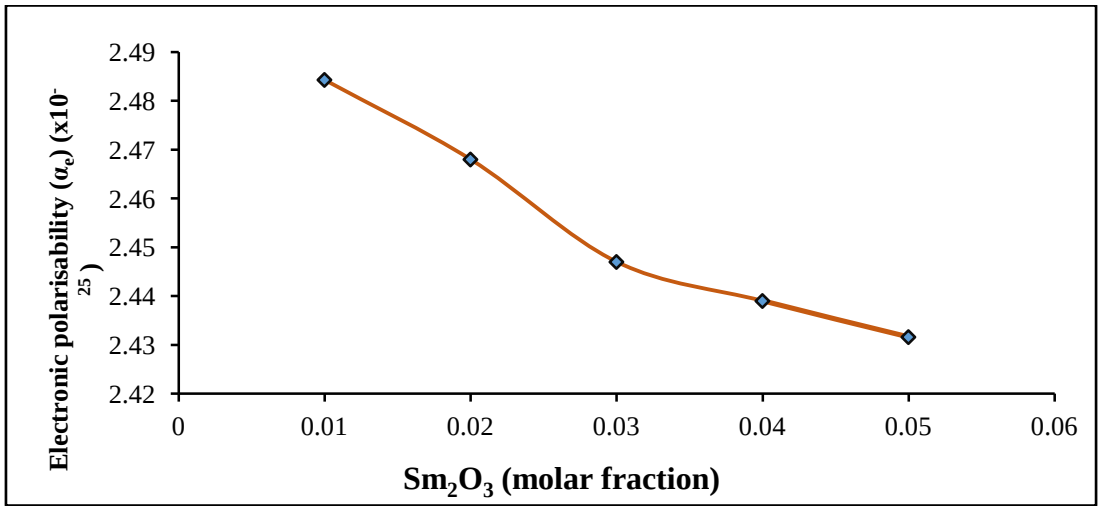

Fig. 13. Plot of electronic polarisability for $[(TeO_2)_{0.7}\ (ZnO)_{0.3}]_{1-x}\ [Sm_2O_3]_x$ glasses

Table 5. Refractive index and electronic polarisability for $[(TeO_2)_{0.7}(ZnO)_{0.3}]_{1-x}[Sm_2O_3]_x$ glasses

Molar fraction (Sm_2O_3)	Refractive index *(n)* [±0.010]	Electronic polarisability (α_e)[±0.009]
0.01	2.457	2.484
0.02	2.439	2.468
0.03	2.416	2.447
0.04	2.408	2.439
0.05	2.400	2.431

6. OXIDE ION POLARISABILITY

Dimitrov and Sakka (1996) have originally proposed the oxide ion electronic polarisability relation for simple oxide and the relation was later stretched to numerous binary glasses by Banu and Jagannathan [24] as well as Dimitrov and Komatsu (2010). The values of No_{2-} is given by $X_1 i + X_2 j + X_3 k + X_4 l$ and $\sum \alpha_i$ are given by $X_1 k\alpha_A + X_2 m\alpha_B + X_3 n\alpha_c + X_4 o\alpha_D$ [20]. The molar cation polarisability for every element in the glass matrix can be obtained from the Komatsu and Dimitrov data of molar cation polarisability [25]. Therefore, the values of the molar cation polarisability of Te^{4+}, Zn^{3+}, and Sm^{3+} ions are as follows: α_{Zn} = 0.283 Å^3, α_{Te} =1.595 Å^3 and α_{Sm} =1.16 Å^3 respectively. The energy band gap and refractive index-based oxide ion polarisabilities decrease with an increase in dopant concentration. The decreasing values can be related to the reduction in the amount of NBOs as the dopant content increases in the glass system [2]. The values of $\alpha_{o2-}(n)$ and $\alpha_{o2-}(E_g)$ of the glass system are calculated and listed in Table 6 while the graph for oxide ion polarisability based on the index of refraction and band gap energy against the dopant concentration is presented in Fig. 14.

7. OPTICAL BASICITY

"The ability of the oxide glasses in contributing negative charges in the glass matrix is determined by the optical basicity of the glass material which is also known as the electron-donating power of the oxygen in the oxide glasses" [26]. According to literature, the optical basicity values for individual oxide are given as : $\Lambda(TeO_2)$ = 0.9300, $\Lambda(ZnO)$ = 1.0800 and $\Lambda(Sm_2O_3)$ = 0.9476 [1]. The theoretical optical basicity increases perfectly indicating the trend of optical basicity values according to[29]. The values for index of refraction based optical basicity, n and band gap energy, E_g decreases which shows the acidic nature of the prepared glasses [2]. Another reason explaining the decreasing optical basicity based on both refractive index and energy band gap is the decreasing number of negative charges on the oxygen atoms which resulted in the reduction of the oxygen bonding covalency in the cation of the glass system [26]. The idea behind the theoretical basicity was only to forecast the trends of optical basicity instead of obtaining the true optical basicity values of the glass system as reported by [29]. The variation between the theoretical optical basicity Λ_{th} and the experimental optical basicity might be due to the significant structural changes in the samples [29]. The values for theoretical optical basicity, refractive index-based optical basicity and energy band gap-based optical basicity are listed in Table 7 and presented in Figures 15 and 16 respectively.

8. METALLIZATION CRITERION

To find out the possibility for glass materials in undergoing metallization and also to study the insulating behaviour of the glass system, the metallization criterion of the glass samples are calculated theoretically [2]. The metallization criterion theory of condensed matter has been

Table 6. Oxide ion polarisability for $[(TeO_2)_{0.7}(ZnO)_{0.3}]_{1-x}[Sm_2O_3]_x$ glasses

Molar fraction (Sm_2O_3)	Refractive index-based oxide ion polarisability, $\alpha_{o2-}(n)$	Energy band gap-based oxide Ion polarisability, $\alpha_{o2-}(E_g)$
0.01	3.273	3.274
0.02	3.237	3.238
0.03	3.208	3.208
0.04	3.154	3.155
0.05	3.107	3.107

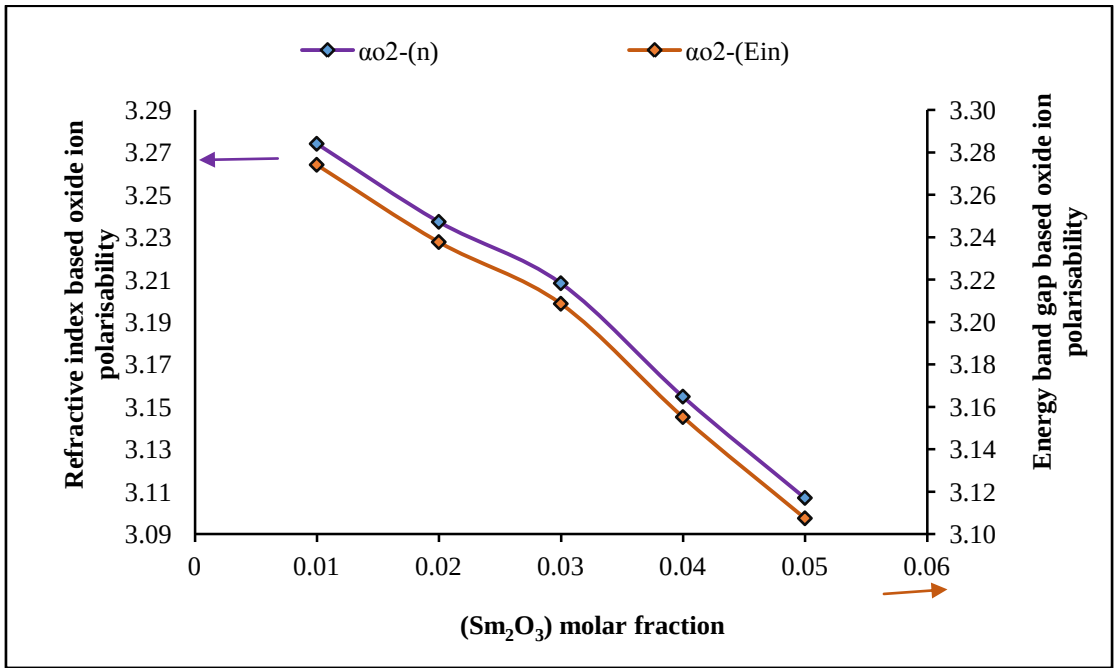

Fig. 14. Oxide ion polarisability for $[(TeO_2)_{0.7}\ (ZnO)_{\ 0.3}]_{1-x}\ [Sm_2O_3]_{\ x}$ glasses

Table 7. Optical basicity for $[(TeO_2)_{0.7}\ (ZnO)_{\ 0.3}]_{1-x}\ [Sm_2O_3]_{\ x}$ glasses

Molar fraction (Sm_2O_3)	Theoretical Optical basicity, (Λ_{th})	Refractive index based optical basicity, $\Lambda(n)$	Energy band gap based optical basicity, $\Lambda(E_g)$
0.01	1.638	1.160	1.161
0.02	1.650	1.154	1.155
0.03	1.662	1.149	1.149
0.04	1.674	1.141	1.142
0.05	1.686	1.133	1.133

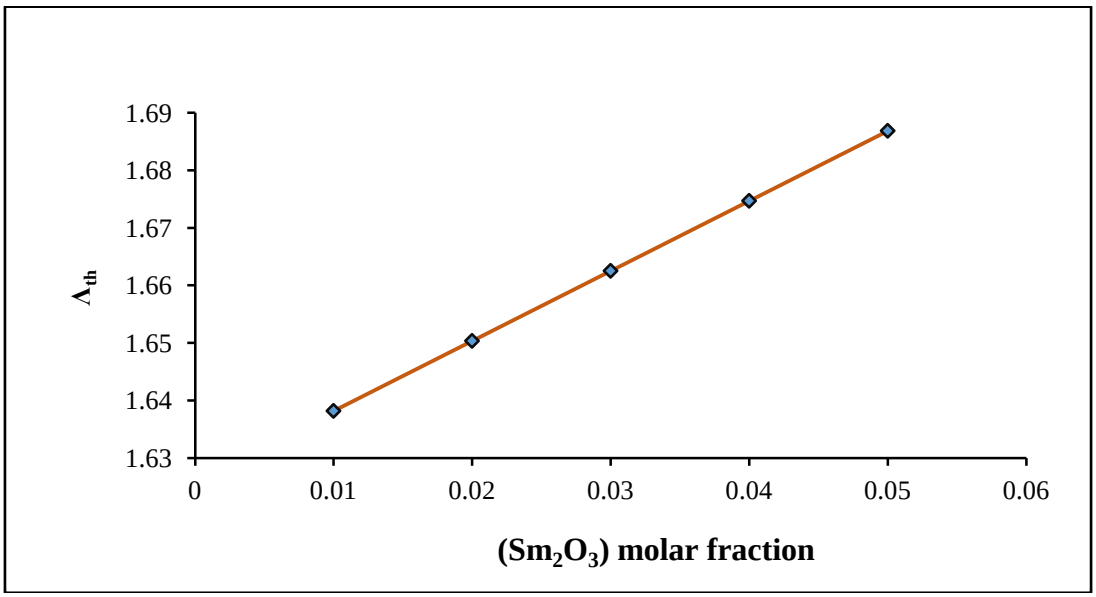

Fig. 15. Theoretical optical basicity for $[(TeO_2)_{0.7}\ (ZnO)_{\ 0.3}]_{1-x}\ [Sm_2O_3]$ x glasses

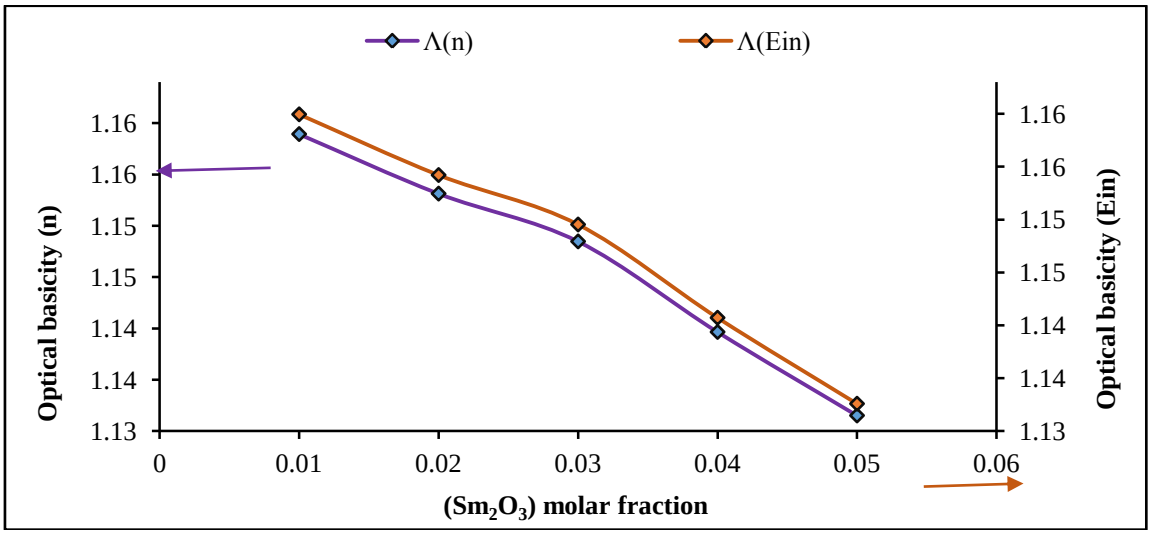

Fig. 16. Optical basicity for $[(TeO_2)_{0.7}\ (ZnO)_{\ 0.3}]_{1-x}\ [Sm_2O_3]\ x$ glasses

Table 8. Refractive index and energy band gap-based metallization criterion for $[(TeO_2)_{0.7}\ (ZnO)_{\ 0.3}]_{1-x}\ [Sm_2O_3]_{\ x}$ glasses

Molar fraction (Sm_2O_3)	Metallization criterion based refractive index, M (n_o)	Metallization criterion-based energy band gap, M (E_g)
0.01	0.373	0.374
0.02	0.377	0.378
0.03	0.383	0.383
0.04	0.385	0.386
0.05	0.387	0.387

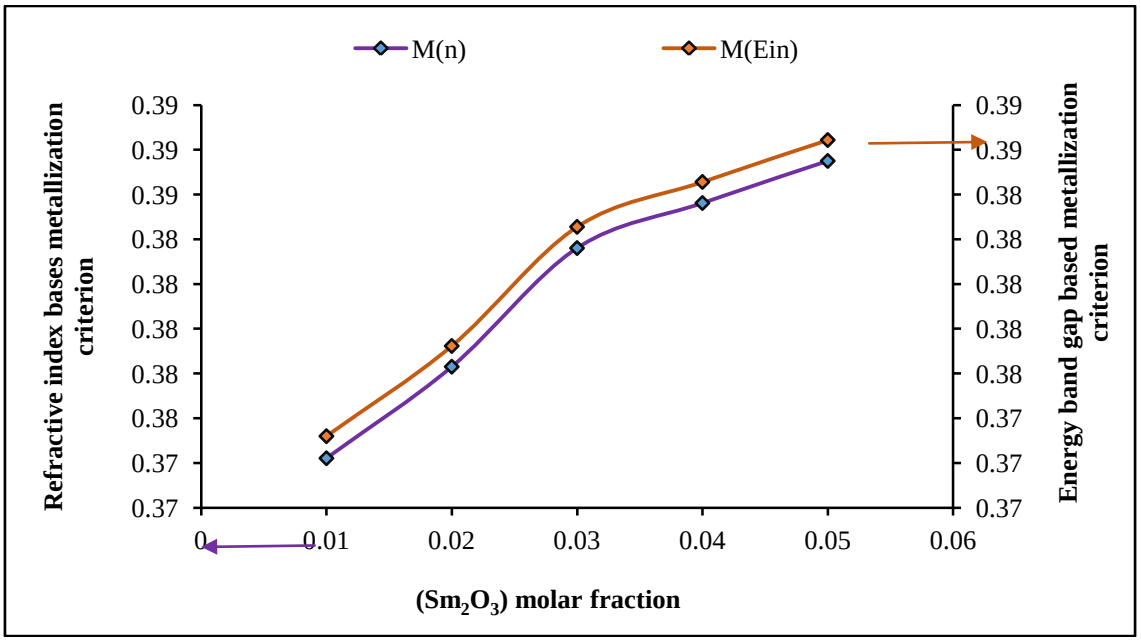

Fig. 17. Metallization criterion based refractive index and band gap energy for $[(TeO_2)_{0.7}\ (ZnO)_{\ 0.3}]_{1-x}\ [Sm_2O_3]\ x$ glasses

suggested by Herzfeld which disclosed that the index of refraction of a glass system is infinite if and only if the relation $R_m/V_m = 1$ in the equation of Lorenz-Lorenz [30]. The theory has stated that any material with the condition of $R_m/V_m \geq 1$ will have a mobile electron and the material is assumed to be metallic in nature while the materials with the condition of $R_m/V_m < 1$ are assumed to be non-metallic in nature [31]. The values for index of refraction-based metallization criterion, $M(n_o)$ and band gap energy-based metallization criterion $M(E_g)$ for the sample glasses are calculated by employing equation (12) and equation (13). The metallization criterion-based refractive index and band gap energy show a perfect increasing trend as samarium oxide concentration increases. The increase in both the metallization criterion signifies that the sample's metalizing tendency is low with high Sm_2O_3 content. The increasing metallization criterion on the band gap energy-based revealed that the glass samples are not metalizing hence the smaller width of the conduction band of the glass system [32]. The calculated metallization criterion values are listed in Table 8 and presented in Fig. 17.

9. CONCLUSION

In conclusion, zinc tellurite glass system doped with Sm^{3+} ions containing chemical formula $[(TeO_2)_{0.7}\ (ZnO)_{0.3}]_{1-x}\ [Sm_2O_3]_x$, where x = 0.01, 0.02, 0.03, 0.04 and 0.05 molar fraction were fabricated using conventional melt quenching technique. The XRD study reveals that there is no sharp peak indicating that the samples being prepared are in the amorphous nature of the state. FTIR investigation shows TeO_4 units exist. The density of the glass system shows an increasing trend. This action can be due to the introduction of modifier oxide which breaks up the Te-O-Te linkage and the free space within the glass network increases. The increase in bandgap reflected the formation of (BOs) in the glass matrix. The decreasing trend of Urbach energy reflects a decrease in the concentration of defects in the glass network and this has also confirmed a higher tendency for the samples to minimize static disorder within their structure. The decline in refractive index and electronic polarisability is due to the decreasing amount of non-bridging oxygen high polarisability in the glass network. The decreasing optical basicity indicates that the sample glasses are more acidic. The increasing refractive index and band gap energy base metallization criterion show that the possibility of the fabricated glasses to metalize is considerably high.

DISCLAIMER

The products used for this research are commonly and predominantly use products in our area of research and country. There is absolutely no conflict of interest between the authors and producers of the products because we do not intend to use these products as an avenue for any litigation but for the advancement of knowledge. Also, the research was not funded by the producing company rather it was funded by personal efforts of the authors.

ACKNOWLEDGEMENT

The research was reinforced by the Malaysian Ministry of Higher Education and University Putra Malaysia (UPM), Malaysia using Geran Putra Berimpak (vot no. 9597200).

COMPETING INTERESTS

Authors have declared that no competing interests exist.

REFERENCES

1. Zhao X, Wang X, Lin H, Wang Z. Correlation among electronic polarizability, optical basicity and interaction parameter of Bi2O3-B2O3glasses," Phys. B Condens. Matter. 2007;390(1–2):293–300,
2. Halimah MK, Faznny MF, Azlan MN, Sidek HAA. Optical basicity and electronic polarizability of zinc borotellurite glass doped La3+ions. Results Phys. 2017;7:581–589.
3. Pavani PG, Sadhana K, Mouli VC. Optical, physical and structural studies of boro-zinc tellurite glasses," Phys. B Phys. Condens. Matter. 2011;406O(6–7):1242–1247.
4. Bhatia B, Meena SL, Parihar V, Poonia M. Optical Basicity and Polarizability of Nd 3 + -Doped Bismuth Borate Glasses. New J. Glas. Ceram. 2015;5:44–52.
5. Usman A, Halimah MK, Latif AA, Muhammad FD, Abubakar AI. Influence of Ho3 +ions on structural and optical properties of zinc borotellurite glass system. J. Non. Cryst. Solids. 2017;483:18–25, 2018.
6. Umar S, Halimah MK, Chan KT, Latif A. Polarizability, optical basicity and electric susceptibility of Er 3 + doped silicate borotellurite glasses," J. Non. Cryst. Solids. 2017;471:101–109.
7. Hager IZ, El-Mallawany R. Preparation and

structural studies in the (70 − x)TeO2–20WO3–10Li2O–xLn2O3 glasses. J. Mater. Sci. 2010;45(4):897–905.
8. Faznny MF, Halimah MK, Azlan MN. Effect of lanthanum oxide on optical properties of zinc borotellurite glass system. Optoelectron. Biomed. Mater. 2016;8(2):49–59.
9. Hajer SS, Halimah MK, Azmi Z, Azlan MN. Optical properties of zinc-borotellurite doped samarium," Chalcogenide Lett. 2014;11(11):553–566.
10. Abdulbaset AA, Halimah MK, Azlan MN. Effect of Neodymium Ions on Density and Elastic Properties of Zinc Tellurite Glass Systems," Solid State Phenom. 2017;268:28–32.
11. Halimaha MK, Hasnimulyati L, Zakaria A, Halim SA, Ishak M, Azuraida A, Al-Hada NM, Influence of gamma radiation on the structural and optical properties of thulium-doped glass. Mater. Sci. Eng. B Solid-State Mater. Adv. Technol. 2017;226:158–163.
12. Tanko YA, Sahar MR, Ghoshal SK. Prominent spectral features of Sm3+ion in disordered zinc tellurite glass. Results Phys. 2016;6:7–11.
13. Linda D, Duclère JR, Hayakawa T, Colas MD, Cardinal T, Mirgorodsky A, Kabadou P. Thomas, Optical properties of tellurite glasses elaborated within the TeO_2 – Tl_2O – Ag_2O and TeO_2 – ZnO – Ag_2O ternary systems. 2013;561:151–160.
14. Eraiah B. Optical properties of samarium doped zinc – tellurite glasses. Bull. Mater. Sci. 2006;29(4):375–378.
15. Widanarto W, Sahar MR, Ghoshal SK, Arifin R, Rohani MS, Hamzah K. Effect of natural Fe_3O_4 nanoparticles on structural and optical properties of Er3+doped tellurite glass," J. Magn. Magn. Mater. 2013;326:123–128.
16. Stambouli W, Elhouichet H, Ferid M. Study of thermal, structural and optical properties of tellurite glass with different TiO2composition. J. Mol. Struct. 2012;1028:39–43.
17. Gautam CR, Das S, Gautam SS, Madheshiya A, Singh AK. Processing and optical characterization of lead calcium titanate borosilicate glass doped with germanium. J. Phys. Chem. Solids. 2018;115:180–186.
18. El-Mallawany R, Abdalla MD, Ahmed IA. New tellurite glass: Optical properties. Mater. Chem. Phys. 2008;109(2–3):291–296.
19. Halimah MK, Daud WM, Sidek HAA, Zaidan AW, Zainal AS. Optical properties of ternary tellurite glasses," Mater. Sci. Pol. 2010;28(1):173–180.
20. M. N. Azlan, M.K. Halimah, S.A . Shafinas, W. M. Daud, "polarizability and optical basicity of er 3 + ions doped tellurite based glasses," Chalcogenide Lett., vol. 11, no. 7, pp. 319–335, 2014.
21. Dimitrov V, Sakka D. Linear and non linear optical properties of simple oxides II. J. Appl. Phys. 1996;79:1741–5.
22. Ayuni JN, Halimah MK, Talib ZA, Sidek HAA, Daud WM, Zaidan AW, Khamirul AM. Optical properties of ternary TeO_2-B_2O_3-ZnO glass system. IOP Conf. Ser. Mater. Sci. Eng. 2011;17(1).
23. Hajer SS, Halimah MK, Azmi Z, Azlan MN. Optical properties of Zinc-Borotellurite doped samarium," Chalcogenide Lett. 2014;11(11):553–566.
24. TB, Vithal RJM, Nachimuthu P. Optical and electrical properties of PbO-TiO2, PbO-eO2 and PbO-Cdo glass systems. J. Appl. Phys. 1997;81(7922).
25. Dimitrov V, Komatsu T. Classification of oxide glasses: A polarizability approach. J. Solid State Chem. 2005;178(3):831–846.
26. Bhatia B, Meena SL, Parihar V, Poonia M. Optical Basicity and Polarizability of Nd 3 + -Doped Bismuth Borate Glasses," New J. Glas. Ceram. 2015;5:44–52.
27. Azlan MN, Halimah MK, Shafinas SZ, Daud WM. Electronic polarizability of zinc borotellurite glass system containing erbium nanoparticles," Mater. Express. 2015;5(3):211–218,
28. Saddeek YB, Shaaban ER, Moustafa ES, Moustafa HM. Spectroscopic properties, electronic polarizability, and optical basicity of Bi2O3-Li2O-B2O3 glasses," Phys. B Condens. Matter. 2008;403(13–16):2399–2407,
29. Duffy JA, Ingram MD. Comments on the application of optical basicity to glass. J. Non. Cryst. Solids. 1992;144©:76–80.
30. Herzfeld KF. On Atomic Properties which make an Element a Metal. Phys. Rev. 1927;29(5):701–705.
31. Honma T, Sato R, Benino Y, Komatsu T, Dimitrov V. Electronic polarizability, optical basicity and XPS spectra of Sb2O3-B2O3glasses," J. Non. Cryst. Solids. 2000;272(1):1–13.
32. Dimitrov V, Komatsu T. An Interpretation of Optical Properties of Oxides and Oxide

Glasses in Terms of the Electronic Ion Polarizability and Average Single Bond Strength (Review). J. Univ. Chem. Technol. Metall. 2010;453:219–250.

Peer-review history:
The peer review history for this paper can be accessed here:
https://www.sdiarticle5.com/review-history/86675